PHYSICAL REVIEW A **82**, 010103(R) (2010)

$\mathcal{PT}$ optical lattices and universality in beam dynamics

Mei C. Zheng,[1] Demetrios N. Christodoulides,[2] Ragnar Fleischmann,[3] and Tsampikos Kottos[1]
[1]*Department of Physics, Wesleyan University, Middletown, Connecticut 06459, USA*
[2]*Center for Research and Education in Optics and Lasers (CREOL), College of Optics and Photonics, University of Central Florida, Orlando, Florida 32816, USA*
[3]*Max-Planck-Institute for Dynamics and Self-Organization, Bunsenstraße 10, D-37073 Göttingen, Germany*
(Received 4 January 2010; published 29 July 2010)

Beam dynamics in synthetic optical media with $\mathcal{PT}$ symmetries imposed by a balanced arrangement of gain or loss is investigated. We find that the beam power evolution is insensitive to microscopic details of the system and that it follows three distinct universal laws which depend only on the magnitude of the gain or loss parameter. Our theoretical calculations are confirmed numerically for the experimentally realizable case of a lattice consisting of coupled $\mathcal{PT}$-symmetric dimers.

DOI: 10.1103/PhysRevA.82.010103 PACS number(s): 42.25.Bs, 11.30.Er, 42.82.Et

Introduction. Systems exhibiting parity-time ($\mathcal{PT}$) symmetry have been the subject of rather intense research activity during the last few years. This interest is motivated by various areas, ranging from mathematical physics [1–3], solid-state [4,5] and atomic physics [6], to linear and nonlinear optics [7–14]. A surprising result that was pointed out in some of these investigations is the possibility that a $\mathcal{PT}$-symmetric Hamiltonian $\mathcal{H}$ can have a real eigenvalue spectrum, even if it is non-Hermitian [2]. The departure from Hermiticity is due to the presence of various gain and loss mechanisms that occur in a balanced manner, so that the net loss or gain of "particles" is zero. Furthermore, because some gain or loss parameter γ that controls the degree of non-Hermiticity of $\mathcal{H}$ gets a critical value $\gamma_{\mathcal{PT}}$, a spontaneous $\mathcal{PT}$-symmetry breaking can occur. For $\gamma > \gamma_{\mathcal{PT}}$, the eigenfunctions of $\mathcal{H}$ cease to be the eigenfunctions of the $\mathcal{PT}$ operator despite the fact that $\mathcal{H}$ and the $\mathcal{PT}$ operator commute [2]. This happens because the $\mathcal{PT}$ operator is antilinear, and thus the eigenstates of $\mathcal{H}$ may or may not be eigenstates of $\mathcal{PT}$. As a consequence, in the *broken* $\mathcal{PT}$-symmetric phase, the spectrum becomes partially or completely complex. The other limiting case, where both $\mathcal{H}$ and $\mathcal{PT}$ share the same set of eigenvectors, corresponds to the so-called *exact* $\mathcal{PT}$-symmetric phase, in which the spectrum is real.

A promising application of $\mathcal{PT}$-symmetric systems appears in the frame of optics, where a medium with alternating regions of gain and loss can be synthesized, provided that the (complex) refractive index profile satisfies the condition $n^*(-x) = n(x)$ [8,9]. Experimental realizations of such systems have been reported in Refs. [11,12] where a simple $\mathcal{PT}$ dimer was created and the beam dynamics was investigated. This kind of synthetic $\mathcal{PT}$ material was shown to exhibit unique characteristics such as power oscillations, loss induced optical transparency, etc. Given that even a single $\mathcal{PT}$ cell can exhibit unconventional features, one may naturally ask what new behavior and properties could be expected from $\mathcal{PT}$ lattices. Numerical simulations [8] indicated that periodic extended systems show "double refraction" and nonreciprocal diffraction patterns, properties that may allow the use of $\mathcal{PT}$ optical lattices as a new generation of unidirectional optical couplers or left-right sensors for propagating light [8]. However, a theoretical understanding of the beam dynamics at the global level is still lacking. At the same time, the effect of (experimentally unavoidable) imperfections in the properties of $\mathcal{PT}$ systems has only very recently been investigated, and only in the frame of spectral statistics [5,13]. In contrast, the study of eigenstates and beam dynamics has been totally unexplored.

Here, we present a theoretical analysis of optical beam behavior in an extended $\mathcal{PT}$ system. Motivated by the experimental realization of Refs. [11,12], we consider as an example case, a lattice consisting of N coupled $\mathcal{PT}$ dimer cells with intradimer and interdimer couplings k and c, respectively. Our analysis will address not only the periodic lattice but also the case in which both c and k are random [13]. Specifically we have found that the beam power $P(z)$ of the propagating light behaves as

$$P(z) \sim \begin{cases} \bar{K} & \text{for } \gamma < \gamma_{\mathcal{PT}}, \\ z^2 & \text{for } \gamma = \gamma_{\mathcal{PT}}, \\ \exp\left(2\sqrt{\gamma^2 - \gamma_{\mathcal{PT}}^2}\, z\right) & \text{for } \gamma > \gamma_{\mathcal{PT}}, \end{cases} \tag{1}$$

where z is the axial propagation distance in the optical array and $\bar{K} = (1/2N)\sum_n \langle R_n|R_n\rangle\langle L_n|L_n\rangle$ is the average diagonal Petermann factor defined via the left $\{\langle L_n|\}$ and right $\{|R_n\rangle\}$ eigenvectors of $\mathcal{H}$. Equation (1) is general and applicable to any system with antilinear (like the $\mathcal{PT}$) symmetry [15].

Model. We consider a one-dimensional (1D) array of coupled optical waveguides. Each of the waveguides can support only one mode, while light is transferred from waveguide to waveguide through optical tunneling. The array consist of two types of waveguides: type A is made from gain material, whereas type B exhibits the equal amount of loss. Their arrangement in space is such that they form N coupled (A-B) dimers with intradimer and interdimer couplings k and c, respectively. In the tight binding description, the diffraction dynamics of the mode electric field amplitude $\Psi_n = (a_n, b_n)^T$ at the nth dimer evolves according to the following Schrödinger-like equation:

$$\begin{aligned} i\frac{da_n(z)}{dz} &= \epsilon a_n(z) + k b_n(z) + c b_{n-1}(z), \\ i\frac{db_n(z)}{dz} &= \epsilon^* b_n(z) + k a_n(z) + c a_{n+1}(z), \end{aligned} \tag{2}$$

where $\epsilon = \epsilon_0 + i\gamma$ is related to the complex refractive index [8]. Without loss of generality, we will assume below that $\epsilon_0 = 0$ and $\gamma > 0$. The coupling terms $(c,k) = (c_0,k_0)$ can be either constant (i.e., fixed distance between the waveguides) or random due to positional disorder in the waveguide arrangement. In this case, we will assume that both are taken from a box distribution of width w, i.e., $c \in [c_0 - w/2; c_0 + w/2]$ and $k \in [k_0 - w/2; k_0 + w/2]$, such that $k_0 - c_0 > w$. We note that if (c,k) are random, the array is no longer $\mathcal{PT}$ symmetric. However, the effective Hamiltonian that describes the system commutes with an antilinear operator (in [13] we coined this $\mathcal{P}_d\mathcal{T}$ symmetry) which is related with the local $\mathcal{PT}$ symmetry of each individual dimer.

Spectral analysis and statistics of $\gamma_{\mathcal{PT}}$. It is instructive to start with the simple, exactly solvable system of N coupled dimers with constant couplings c_0,k_0. To this end, we write the field amplitudes (a_n,b_n) in their Fourier representation, i.e., $a_n(z) = \frac{1}{2\pi}\int_{-\pi}^{\pi} dq \tilde{a}_q(z)\exp(inq)$ (and similarly for b_n). Substitution to Eq. (2) leads to

$$i\frac{d}{dz}\begin{pmatrix}\tilde{a}_q(z)\\ \tilde{b}_q(z)\end{pmatrix} = H_q\begin{pmatrix}\tilde{a}_q(z)\\ \tilde{b}_q(z)\end{pmatrix}, \quad H_q = \begin{pmatrix}\epsilon & v\\ v^* & \epsilon^*\end{pmatrix}, \tag{3}$$

where $v = k + ce^{-iq}$. Substituting in Eq. (3) the stationary form $(a_n,b_n)^T = \exp(-i\mathcal{E}z)(A,B)^T$, we get

$$\mathcal{E}\begin{pmatrix}A\\ B\end{pmatrix} = \begin{pmatrix}\epsilon & v\\ v^* & \epsilon^*\end{pmatrix}\begin{pmatrix}A\\ B\end{pmatrix}. \tag{4}$$

The spectrum is obtained by requesting a nontrivial solution, i.e., $(A,B) \neq 0$. In this case, we obtain the band structure of this diatomic $\mathcal{PT}$ system:

$$\mathcal{E}(q) = \pm\sqrt{k^2 + c^2 + 2kc\cos(q) - \gamma^2}, \quad q \in [-\pi,\pi]. \tag{5}$$

For $\gamma = 0$ we have two bands of width $2c$, centered at $\mathcal{E} = \pm k$. In the following, we will assume that $k > c$. In this case, the two bands are separated by a gap $\delta = 2(k - c)$ and the exact $\mathcal{PT}$ phase extends over a large γ regime. However, for $k \leqslant c$, the critical value $\gamma_{\mathcal{PT}}$ is exponentially small (with respect to the system size) due to the existence of surface states [5,16].

As γ increases beyond $\gamma_{\mathcal{PT}}$ the spectrum becomes partially complex. The mechanism for this breaking is level crossing between levels (corresponding to $q = \pi$) belonging to different bands [13]: it follows from Eq. (5) that when $\gamma = \gamma_{\mathcal{PT}} = \delta/2$, the gap disappears and the two (real) levels at the "inner" band edges become degenerate; for $\gamma > \gamma_{\mathcal{PT}}$, they branch out into the complex plane, displaying the characteristic behavior [5,13]

$$\Im[\mathcal{E}(q = \pi)] = \pm\sqrt{\gamma^2 - \gamma_{\mathcal{PT}}^2}; \quad \gamma_{\mathcal{PT}} = k - c. \tag{6}$$

It turns out that the same scenario for the transition from the exact to the broken phase applies for the case of random couplings k,c as well (see the upper inset of Fig. 1) [13]. At the main panel of Fig. 1, we show our numerical data for the average $\langle\gamma_{\mathcal{PT}}\rangle$ for various $(k_0;c_0;N;w)$ values by making use of the scaled variables

$$\langle\gamma_{\mathcal{PT}}\rangle/c_0 = x - 1, \qquad x = k_0/c_0, \tag{7}$$

which are inspired by Eq. (6). For each point, an ensemble of a considerable number of different disorder realizations (at least 10^4) has been used. From each realization, we have identified

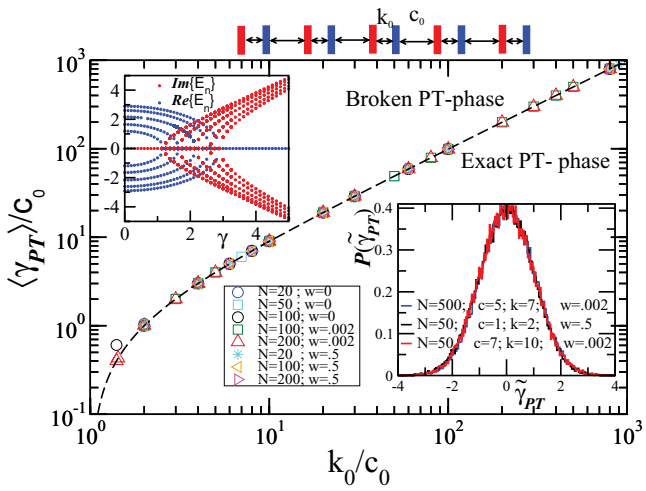

FIG. 1. (Color online) Realization of the system of Eq. (2) is shown in the upper part of the figure: the red blocks represent waveguides with amplification, while the blue blocks are waveguides with absorption. Main panel: The average $\langle\gamma_{\mathcal{PT}}\rangle/c_0$ vs k_0/c_0 for various system sizes $2N$ and disorder strengths w. The dashed line represents the theoretical prediction Eq. (7). Upper inset: The bifurcation diagram of an array of $N = 5$ dimers, with $(k_0,c_0) = (2,1)$ and $w = 0.002$. The spontaneous $\mathcal{PT}$-symmetry breaking is a result of a level crossing between the two closest levels that belong to different bands. Lower inset: Gaussian distribution $\mathcal{P}(\tilde{\gamma}_{\mathcal{PT}})$ of the scaled parameter $\tilde{\gamma}_{\mathcal{PT}} \equiv (\gamma_{\mathcal{PT}} - \langle\gamma_{\mathcal{PT}}\rangle)/\sigma$ (σ^2 is the variance) for various system sizes, disordered strengths w, and $(k_0;c_0)$ values.

$\gamma_{\mathcal{PT}}$ which was used in our analysis. The agreement between our data and Eq. (7) is evident.

We study now the distribution of $\gamma_{\mathcal{PT}}$. The latter (even in the case of disorder) is $\gamma_{\mathcal{PT}} = \delta/2$, where δ is the size of the band gap. We invoke perturbation theory with respect to the perfect lattice. The perturbative scenario indicates that weak disorder will cause a small shift of the levels. Thus the new band gap is $\delta \pm \Delta\delta$. The correction in first-order perturbation theory is $\Delta\delta \sim \sum_{n=1}^{N-1}(A_nB_n\delta k_n + A_{n+1}B_n\delta c_{n+1})$, with the coefficients $A_n = A\sin(\frac{2\pi Nn}{2N+1})$ and $B_n = B\sin(\frac{2\pi Nn}{2N+1})$. If δk_n and δc_n were Gaussian distributed, it would be immediately clear that the distribution of $\tilde{\gamma}_{\mathcal{PT}} \equiv (\gamma_{\mathcal{PT}} - \langle\gamma_{\mathcal{PT}}\rangle)/\sigma = \Delta\delta/\sigma$, $P(\tilde{\gamma}_{\mathcal{PT}})$, is a Gaussian ($\sigma^2 = w^2/12$ is the variance of the box distribution). This should remain approximately true also for the box distribution, employed in our numerics for sufficiently large number of terms in the sum. The lower inset of Fig. 1 confirms this expectation.

Eigenvector statistics. The eigenvectors of a non-Hermitian system are biorthogonal, and therefore they do not respect the standard (Euclidian) orthonormalization condition. Let $\langle L_n|$ and $|R_n\rangle$ denote the left and right eigenvectors of the non-Hermitian Hamiltonian $\mathcal{H}$ corresponding to the eigenvalue $\mathcal{E}_n = E_n + i\Gamma_n$, i.e., $\langle L_n|\mathcal{H} = \langle L_n|\mathcal{E}_n$ and $\mathcal{H}|R_n\rangle = \mathcal{E}_n|R_n\rangle$. The vectors can be normalized to satisfy $\langle L_n|R_m\rangle = \delta_{nm}$, while $\sum_n |R_n\rangle\langle L_n| = 1$. An important observable that measures the nonorthogonality of the modes (and consequently the degree of non-Hermiticity of the system) is the so-called Petermann factor, defined as $K_{nm} = \langle L_n|L_m\rangle\langle R_m|R_n\rangle$ [17]. Here we study

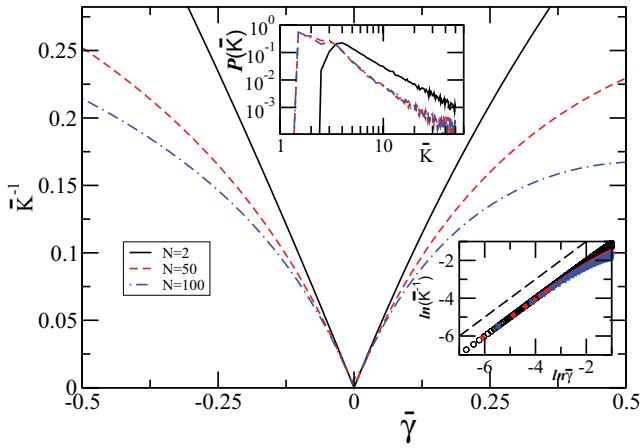

FIG. 2. (Color online) Inverse Petermann factor $1/\bar{K}$ as a function of $\bar{\gamma} \equiv (\gamma - \gamma_{\mathcal{PT}})\mathcal{N}$ for various systems sizes $\mathcal{N}$. Upper inset figure: Distribution of the Petermann factors $\mathcal{P}(\bar{K})$ close to the critical point $\gamma_{\mathcal{PT}}$. Lower inset figure: Dependence of $\bar{K}^{-1}$ from $\bar{\gamma}$ close to the critical point. The data are reported in a double-logarithmic fashion. The dashed line has slope -1 and is drawn to guide the eye.

the mean (diagonal) Petermann factor of our disordered dimer chains of length $\mathcal{N} = 2N$:

$$\overline{K}_N = \frac{1}{\mathcal{N}} \sum_{n=1}^{\mathcal{N}} K_{nn} = \frac{1}{\mathcal{N}} \sum_{n=1}^{\mathcal{N}} \langle L_n | L_n \rangle \langle R_n | R_n \rangle, \tag{8}$$

which takes the value of unity if the eigenfunctions of the system are orthogonal, while it is larger than unity in the opposite case. It has been shown that the Petermann factor can diverge at exceptional points in the spectrum [18,19]. This indicates strong correlations between the spectrum and the eigenvectors which can affect drastically the dynamics as we will see later. We conjecture that the anomalous behavior of $\overline{K}_N$ near the exceptional points is dominated by the contributions of pairs of $\mathcal{PT}$-symmetric states in the vicinity of these points. These pairs form effective dimers with a coupling k. The mean Petermann factor of the single dimer $\overline{K}_2$ is found to be

$$\overline{K}_2 = \frac{(\gamma + k + |\gamma - k|)^2}{4(\gamma + k)|\gamma - k|}. \tag{9}$$

Figure 2 shows our numerical data for $\langle \overline{K}_N \rangle^{-1}$ (where $\langle \cdots \rangle$ indicates an additional averaging over different disorder realizations), for different system sizes near the first exceptional point occurring at $\gamma_{\mathcal{PT}}$. The good agreement with Eq. (9) confirms the validity of our assumption. Furthermore, it allows us to estimate the asymptotic distribution of the Petermann factors for an ensemble of disordered chains. Specifically, using Eq. (9), we find that $P(\overline{K}_N \to \infty) \sim 1/\overline{K}_N^2$. This result agrees perfectly with the numerical data shown in the inset of Fig. 2. We note that the $P(\overline{K}_N)$ found for the case of the $\mathcal{PT}$ Hamiltonians is different from the one reported for the distribution of Petermann factors for the Ginembre ensemble of non-Hermitian random matrices [20].

Dynamics. We turn now to the study of the dynamics of $\mathcal{PT}$ systems; see Fig. 3(a). First, we will give a general argument, based on the behavior of the Petermann factors.

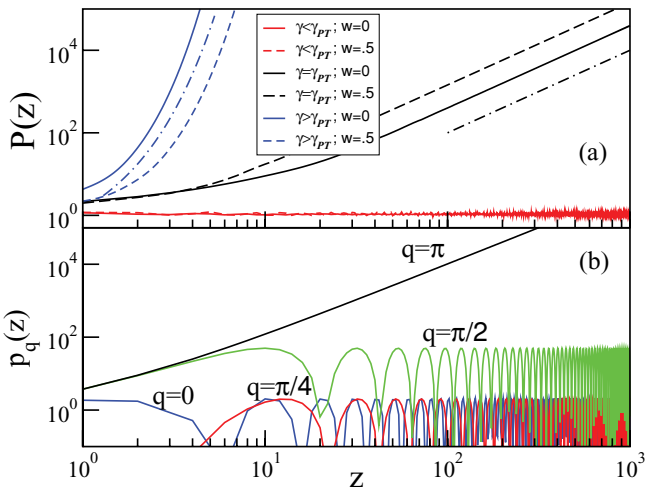

FIG. 3. (Color online) (a) Propagation behavior of the total beam power for three different values of γ and $(c_0; k_0) = (1; 2)$: (a) $\gamma < \gamma_{\mathcal{PT}}$ where $P(z) \approx$ const. for long distances; (b) $\gamma = \gamma_{\mathcal{PT}}$ where $P(z) \sim z^2$ (black dotted-dashed line); and (c) $\gamma > \gamma_{\mathcal{PT}}$ where $P(z) \sim \exp(2\Gamma z)$ with $\Gamma = \sqrt{\gamma^2 - \gamma_{\mathcal{PT}}^2}$ (blue dotted-dashed line). We report the results for both the periodic (solid lines) and disordered dimeric (dashed lines) lattice with $w = 0.5$. (b) The survival probability $p_q(z)$ of representative momentum components for the periodic chain at $\gamma = \gamma_{\mathcal{PT}}$. The $q = \pm\pi$ is responsible for the quadratic evolution of the total power.

We start by writing the evolving beam in terms of left and right eigenvectors of the non-Hermitian Hamiltonian $\mathcal{H}$:

$$|\psi(z)\rangle = e^{-i\mathcal{H}z}|\psi(0)\rangle = \sum_n |R_n\rangle e^{-i\mathcal{E}_n z}\langle L_n|\psi(0)\rangle. \tag{10}$$

Ensemble averaging with $\langle\psi(0)|\psi(0)\rangle = 1$ yields for the total power $P(z)$:

$$P(z) \equiv \overline{\langle\psi(z)|\psi(z)\rangle} = \frac{1}{\mathcal{N}} \sum_{n,m} e^{-i(\mathcal{E}_n - \mathcal{E}_m^*)z} K_{nm}. \tag{11}$$

In the large z limit (and omitting oscillations), one can calculate $P(z)$ using a diagonal approximation

$$P(z) \approx \frac{1}{\mathcal{N}} \sum_n e^{2\Gamma_n z} K_{nn}. \tag{12}$$

If $\gamma < \gamma_{\mathcal{PT}}$, then the eigenvalues $\mathcal{E}_n$ are real, i.e., $\Gamma_n = 0$ and thus $P(z)$ will be given by Eq. (1a). On the other hand, for $\gamma > \gamma_{\mathcal{PT}}$, the dominant term in the sum of Eq. (12) is associated with the level that first breaks the exact phase and acquires an imaginary part given by the positive branch of Eq. (6). This results in an exponential growth[1] of the total power $P(z)$, in agreement with Eq. (1c). Finally, at the transition point $\gamma = \gamma_{\mathcal{PT}}$, the Petermann factor associated with the pair of states that break the exact phase diverge. As a result, the sum in Eq. (12) is dominated by the corresponding term, leading to the conclusion that the temporal behavior of $P(z)$ can be

[1]There are similarities between the behavior of the total beam power of an optical $\mathcal{PT}$-symmetric system and the corresponding one for nonequilibrium plasmas. In the latter case, the exponential power growth is triggered by plasma instabilities due to excess gain [22].

approximated by the dynamics of a two-level system [21] at the $\mathcal{PT}$ transition point. To this end, we write the 2×2 $\mathcal{PT}$ Hamiltonian H [see Eq. (3) with effective coupling $v=k$] in the form $H=\omega\hat{\sigma}\hat{n}$, where $\omega=\sqrt{k^2-\gamma^2}$, $\hat{n}=(1/\omega)(k,0,i\gamma)$, and $\hat{\sigma}$ is a three-component vector of the Pauli matrices. Using the identity $\exp(i\chi\hat{\sigma}\hat{n})=\cos(\chi)\hat{1}+i\sin(\chi)\hat{\sigma}\hat{n}$($\hat{1}$ is the unit matrix), the evolution matrix $\hat{U}$ takes the form

$$\hat{U}=e^{-iHz}=\cos(\omega z)\hat{1}-i\sin(\omega z)\hat{\sigma}\hat{n}. \tag{13}$$

After some straight-forward algebra [16], we find that $P(z)=\langle\psi(0)|\hat{U}^{\dagger}U|\psi(0)\rangle\sim z^2$, in agreement with Eq. (1b).

Let us briefly discuss the dynamics for the simple case of a periodic chain of N coupled dimers. In this case, the evolution can be derived exactly allowing us to see in a transparent way the validity of the main points of our previous general derivation. To this end, one first notes that the two-component wave functions for different q values in Eq. (3) are decoupled, allowing us to evaluate the evolution of the qth momentum component under the 2×2 Hamiltonian H_q. The resulting evolution operator $\hat{U}_q$ can be written in the form [16]

$$\hat{U}_q\equiv e^{-iH_qz}=\cos\left(\frac{1}{2}\omega z\right)\hat{1}-i\sin\left(\frac{1}{2}\omega z\right)\hat{\sigma}\hat{n}, \tag{14}$$

where $\omega=2\sqrt{|v_q|^2-\gamma^2}$, while the unit vector $\hat{n}=\frac{2}{\omega}(|v_q|\cos(q),|v_q|\sin(q),i\gamma)$. By assuming an initial δ-like packet in position space, all components in q space are initially occupied with equal weight. Then, the probability density $p_q(z)\equiv|\tilde{a}_q|^2+|\tilde{b}_q|^2$ to find the system with momentum q at distance z is

$$p_q(z)=\cos^2\left(\frac{\omega z}{2}\right)+\frac{4(\gamma^2+|v_q|^2)}{\omega^2}\sin^2\left(\frac{\omega z}{2}\right). \tag{15}$$

Using Parseval's theorem $\sum_n|\Psi_n(z)|^2=\frac{1}{2\pi}\int_{-\pi}^{\pi}dqp_q(z)$, we get $P(z)$. To this end, one has to note that the q integral is dominated by the $q=\pm\pi$ component which is associated with the pair of levels that first cross, leading to the spontaneous breaking of the $\mathcal{PT}$ symmetry. This pair, for $\gamma=\gamma_{\mathcal{PT}}$, gives us a $p_{\pm\pi}\sim z^2$ behavior [see Fig. 3(b)], while for $\gamma>\gamma_{\mathcal{PT}}$ we get $p_{\pm\pi}\sim\exp(2\Gamma z)$.

Conclusions. We have analyzed the evolution of the beam power $P(z)$ in extended $\mathcal{PT}$ lattices and show that it is independent of the microscopic details (such as disorder or periodicity) of the system. Three universal regimes were identified based on the value of the non-Hermiticity parameter γ: for $\gamma<\gamma_{\mathcal{PT}}$ the total beam power oscillates around some constant; for $\gamma>\gamma_{\mathcal{PT}}$ it increases exponentially; while for $\gamma=\gamma_{\mathcal{PT}}$ it grows quadratically due to the biorthogonal nature of the eigenstates (singularities of the Petermann factor). Our theory was confirmed numerically for an experimentally realizable case of a chain of coupled dimers. Our results will find direct applications in optics where waveguide arrays with $\mathcal{PT}$ symmetries are promising candidates of a new type of synthetic material, with exotic beam propagation properties.

Useful discussions with V. Kovanis are acknowledged. This research was supported by the DFG FOR760, the United States–Israel Binational Science Foundation and a grant from the AFOSR.

[1] C. M. Bender, S. Boettcher, and P. N. Meisinger, J. Math. Phys. **40**, 2201 (1999); C. M. Bender and S. Boettcher, Phys. Rev. Lett. **80**, 5243 (1998).
[2] C. M. Bender, Rep. Prog. Phys. **70**, 947 (2007).
[3] C. M. Bender, D. C. Brody, and H. F. Jones, Phys. Rev. Lett. **89**, 270401 (2002); H. F. Jones, Phys. Lett. A **286**, 231 (2001); J. K. Boyd, J. Math. Phys. **42**, 15 (2001).
[4] N. Hatano and D. R. Nelson, Phys. Rev. Lett. **77**, 570 (1996).
[5] O. Bendix, R. Fleischmann, T. Kottos, and B. Shapiro, Phys. Rev. Lett. **103**, 030402 (2009); C. T. West, T. Kottos, and T. Prosen, *ibid.* **104**, 054102 (2010).
[6] M. Hiller, T. Kottos, and A. Ossipov, Phys. Rev. A **73**, 063625 (2006); E. M. Graefe *et al.*, J. Phys. A **41**, 255206 (2008).
[7] R. El-Ganainy *et al.*, Opt. Lett. **32**, 2632 (2007).
[8] K. G. Makris, R. El-Ganainy, D. N. Christodoulides, and Z. H. Musslimani, Phys. Rev. Lett. **100**, 103904 (2008).
[9] Z. H. Musslimani, K. G. Makris, R. El-Ganainy, and D. N. Christodoulides, Phys. Rev. Lett. **100**, 030402 (2008).
[10] S. Klaiman, U. Günther, and N. Moiseyev, Phys. Rev. Lett. **101**, 080402 (2008).
[11] A. Guo *et al.*, Phys. Rev. Lett. **103**, 093902 (2009).
[12] C. E. Rüter *et al.*, Nature Phys. **6**, 192 (2010).
[13] O. Bendix *et al.*, J. Phys. A **43**, 265305 (2010).
[14] S. Longhi, Phys. Rev. Lett. **103**, 123601 (2009); Phys. Rev. B **80**, 235102 (2009).
[15] For an example of an optical system with antilinear symmetry, see [13]; C. M. Bender, M. V. Berry, and A. Mandilara, J. Phys. A. **35**, L467 (2002).
[16] M. C. Zheng, Honor thesis, Paper 515, Wesleyan University, 2010.
[17] K. Petermann, IEEE J. Quantum Electron. **15**, 566 (1979); A. E. Siegman, Phys. Rev. A **39**, 1264 (1989).
[18] M. V. Berry, J. Mod. Opt. **50**, 63 (2003).
[19] S.-Y. Lee *et al.*, Phys. Rev. A **78**, 015805 (2008).
[20] B. Mehlig and J. T. Chalker, J. Math. Phys. **41**, 3233 (2000).
[21] C. M. Bender, D. C. Brody, H. F. Jones, and B. K. Meister, Phys. Rev. Lett. **98**, 040403 (2007).
[22] A. B. Mikhailovskii, *Theory of Plasma Instabilities* (Plenum, New York, 1974); J. Cen, K. Kempa, and P. Bakshi, Phys. Rev. B **38**, 10051 (1988).